

Boric acid induces cytoplasmic stress granule formation, eIF2 α phosphorylation, and ATF4 in prostate DU-145 cells

Kimberly A. Henderson · Sarah E. Kobylewski ·
Kristin E. Yamada · Curtis D. Eckhert

Received: 8 July 2014 / Accepted: 13 November 2014 / Published online: 26 November 2014
© The Author(s) 2014. This article is published with open access at Springerlink.com

Abstract Dietary boron intake is associated with reduced prostate and lung cancer risk and increased bone mass. Boron is absorbed and circulated as boric acid (BA) and at physiological concentrations is a reversible competitive inhibitor of cyclic ADP ribose, the endogenous agonist of the ryanodine receptor calcium (Ca²⁺) channel, and lowers endoplasmic reticulum (ER) [Ca²⁺]. Low ER [Ca²⁺] has been reported to induce ER stress and activate the eIF2 α /ATF4 pathway. Here we report that treatment of DU-145 prostate cells with physiological levels of BA induces ER stress with the formation of stress granules and mild activation of eIF2 α , GRP78/BiP, and ATF4. Mild activation of eIF2 α and its downstream transcription factor, ATF4, enables cells to reconfigure gene expression to manage stress conditions and mild activation of ATF4 is also required for the differentiation of osteoblast cells. Our results using physiological levels of boric acid identify the eIF2 α /ATF pathway as a plausible mode of action that underpins the reported health effects of dietary boron.

Keywords Boron · Boric acid · eIF2 α · ATF4 · DU-145 cells

Abbreviations

BA	Boric acid
cADPR	Cyclic ADP ribose
ER	Endoplasmic reticulum
TIA-1	T-cell intracellular antigen-1
Grp78	Binding immunoglobulin protein (BiP) also known as 78 kDa glucose-regulated protein
ATF4	Activating transcription factor 4
SG	Stress granule
ISR	Integrated stress response

Introduction

Human boron intake is affected by both regional geology, which contributes to its concentration in drinking water and agricultural soils, and by local preferences for boron rich fruits, vegetables, nuts, legumes and plant based beverages such as coffee, wine and fruit juice (Rainey and Nyquist 1998; Barranco et al. 2007a, b). Higher intake of boron is associated with a lower risk of prostate cancer and volume in men, lung cancer in women, and bone mass in animals (Mahabir et al. 2008; Korkmaz et al. 2007). In humans, 83–98 % of dietary boron is excreted in urine in 96 h and is distributed as boric acid (BA) to all tissues (WHO 1998). Cellular studies at physiological

K. A. Henderson · S. E. Kobylewski ·
K. E. Yamada · C. D. Eckhert
Interdepartmental Program in Molecular Toxicology,
University of California, Los Angeles, CA, USA

C. D. Eckhert (✉)
Department of Environmental Health Sciences, University
of California, Charles E. Young Drive, Los Angeles,
CA 90095, USA
e-mail: ceckhert@ucla.edu

concentrations of BA were made possible by the development of a procedure to deplete BA from cell culture media (Bennett et al. 1999). In healthy men blood BA concentrations range from below a detectable limit of 4.7 μM B (48.5 μg B/g wet blood) in low boron regions to 350 μM B (3,600 μg B/g wet blood) in boron mine workers (Bolt et al. 2012). BA is also a developmental and reproductive toxin with a lowest observed adverse effect level (LOAEL) for testicular damage in rats reported at 620 μM B (Ku et al. 1993; Chapin et al. 1997). The U.S. Environmental Protection Agency set a reference dose (RfD) at 0.2 mg B/kg/d (EPA 2004). BA inhibits the proliferation of LNCaP and DU-145 prostate cancer cells in a dose-dependent manner within the physiological range (Barranco and Eckhert 2004). To identify a functional molecular target of BA in the absence of a stable radioactive boron isotope we based our approach on the knowledge that BA interacts with NAD^+ (Johnson and Smith 1976; Kim et al. 2003, 2004). CD38, a multifunctional enzyme in the plasma membrane, converts extracellular NAD^+ into cyclic ADP ribose (cADPR), the only known agonist of the ryanodine receptor calcium (Ca^{2+}) channel. We identified cADPR as a molecular target of BA and demonstrated that physiological levels of BA inhibit cADPR-activated ER Ca^{2+} release within seconds of treatment and reduce ER luminal Ca^{2+} concentrations ($[\text{Ca}^{2+}]_{\text{ER}}$) (Henderson et al. 2009; Kim et al. 2006).

High $[\text{Ca}^{2+}]_{\text{ER}}$ is required for protein folding in the ER and provides a steep gradient between the ER (100–500 μM) and cytoplasm (20–100 nM) that enables rapid Ca^{2+} signaling (Berridge 1997, 2002). Treatment with thapsigargin, a plant sesquiterpene lactone, inhibits the ATP-dependent ER Ca^{2+} pump (SERCA) resulting in lower $[\text{Ca}^{2+}]_{\text{ER}}$ and accumulation of unfolded and misfolded proteins (Conn 2011; Deniaud et al. 2008). Unfolded proteins sequester glucose-regulated protein (GRP78/BiP) away from the luminal domain of the ER transmembrane protein, double stranded RNA-activated protein kinase (PKR)-like ER kinase (PERK) (Hendershot 2004; Shen et al. 2004). The release of GRP78/BiP enables PERK to dimerize and phosphorylate the serine 51 residue of eukaryotic initiation factor 2 α (eIF2 α). Phosphorylation of eIF2 α mediates the integrated stress response (ISR) which maintains cellular homeostasis under mild ER stress and redirects transcription and translation to a subset of proteins that include the transcription factor

ATF4 which is usually down-regulated in models of human prostate cancer (So et al. 2009). Non-toxic levels of BA have been reported to activate phosphorylation of eIF2 α in mammalian cells (Henderson and Eckhert 2006; Henderson 2009) and teratogenic levels have been reported to activate it in yeast (Uluisik et al. 2011; Narotsky et al. 1998; WHO 1998). Here we report that treatment of DU-145 prostate cancer cells with physiological concentrations of BA causes mild ER stress with ER expansion, the formation of cytoplasmic stress granules, and activation of the eIF2 α /ATF4 integrated stress response (ISR).

Materials and methods

Chemicals

Boric acid, Tris, NaCl, MgCl_2 , sucrose, DTT, methanol, and DMSO were purchased from Sigma-Aldrich (St. Louis, MO). Glutaraldehyde, cacodylic acid, lead citrate, and uranyl acetate were purchased from Electron Microscopy Supplies (Hatfield, PA). Paraformaldehyde was purchased from Affymetrix/USB Corporation (Cleveland, OH). TritonX-100, Tween-20, NP40, and cycloheximide were purchased from Fisher Scientific (Pittsburg, PA). BSA and thapsigargin were purchased from Santa Cruz Biotechnologies (Santa Cruz, CA). Fetal Bovine Serum (FBS) was purchased from Gibco-Life Sciences (Grand Island, NY). Protease and phosphatase inhibitors were purchased from Calbiochem (San Diego, CA).

Cell culture

DU-145 prostate cancer cells, obtained from the American Type Culture Collection (Manassas, VA), were maintained in RPMI Media 1640 (Gibco-Life Technologies, Grand Island, NY) supplemented with 10 % FBS, penicillin (100 U/ml), streptomycin (100 $\mu\text{g}/\text{ml}$), and L-glutamine (200 mM) (Gemini Bio-Products, Sacramento, CA). Cells were plated on 10 or 15 cm plates (Corning Life Sciences, Corning, NY) and incubated at 37 °C in a humidified chamber containing 5 % CO_2 and 95 % air and grown to 80 % confluency. Our procedure to remove boron from media has been previously described (Bennett et al. 1999). All treatment groups in the present study used media that had been stripped of boron by shaking with 2 g of Amberlite IRA 743 exchange resin (Sigma-Aldrich) for 12 h at 4 °C.

Transmission electron microscopy (TEM)

Cells were grown on plastic cover slips (Nalgene, Rochester, NY) to no more than 80 % confluency and treated with BA-supplemented complete media at concentrations of 0, 10, 50, and 250 μM for 24 h, followed by fixation with 2 % glutaraldehyde in 0.1 M sodium cacodylate buffer. Samples were dehydrated with increasing concentrations of ethanol followed by infiltration and embedding in RL White acrylic resin (Ted Pella, Redding, CA). The resin embedded cells were sectioned in 100 nm slices and placed on copper grids. The sections were counter stained with 2 % aqueous uranyl acetate at 57 °C for 1 h followed by 4 % lead citrate staining for 1 min. Imaging by TEM was performed using a JEOL 100CX transmission electron microscope.

Immunofluorescent microscopy

DU-145 cells were grown to 80 % confluency on glass cover slips (Fisher Scientific, Pittsburg, PA) and treated with either BA-free media (0), BA-free media supplemented with BA, or 1 μM thapsigargin. Cells stained for TIA-1 were first fixed with 4 % paraformaldehyde in PBS and permeabilized with 0.5 % TritonX-100 in PBS. Fixed cells were blocked with 10 % FBS in PBS overnight. Next, they were incubated in a humidity chamber with anti-TIA-1 (Santa Cruz Biotechnology) monoclonal antibody at concentrations of 1:50 followed by secondary FITC at 1:100. Coverslips were mounted with a mixture of Vectashield with 4',6-diamidino-2-phenylindole (Vector Laboratories, Burlingame, CA) and regular HardSet Vectashield (Vector Laboratories) mounting mediums at 1:5 respectively. Images were captured with an Olympus DP72 camera (Olympus America, Center Valley, PA) connected to an Olympus BX51 fluorescence microscope (Olympus America) using an Olympus UIS2 UPlanFLN 100X/1.30 OilPh3 objective (Olympus America) and FITC and DAPI filters. Either Olympus DP2-BSW (Olympus America) or Adobe Photoshop (Adobe Systems Incorporated, San Jose, CA) software was used to merge and crop images.

Immunoblot analysis

DU-145 cells grown on 15 cm plates (Corning) to 80 % confluency were treated with BA-free media (0) or BA-free media supplemented with BA, 1 μM thapsigargin, or DMSO positive control vehicle for

varying time points. Cells were washed with ice cold phosphate buffer solution (PBS) supplemented with 0.1 % Tween (PBST) prior to adding 100 μl radio immunoprecipitation assay (RIPA) lysis buffer. Cell lysates were scraped from plates using a spatula (Corning) and passed through a 23 gauge needle (BD, Franklin Lakes, NJ) 8–10 times on ice. The protein was quantitated using the Coomassie Plus Protein Assay (Thermo-Scientific, Waltham, MA). Aliquots of 30–35 μg protein were run on a 4–12 % gradient TGX SDS-PAGE (Bio-Rad, Hercules, CA) at 200 V for 30 min along with a molecular weight ladder (Bio-Rad). Protein was transferred to a nitrocellulose membrane in transfer buffer with 20 % methanol at 40 V for 1.5 h. Membranes were blocked in 3 % BSA with 37.5 mM Tris (pH 8.8), 125 mM NaCl, and 0.1 % Tween 20 for at least 4 h. Following blocking, the membranes were incubated with the primary antibody for 1 h in PBST or 3 % BSA blocking solution, washed in PBST, and incubated with the appropriate secondary antibody with a HRP tag, followed by washing three times with PBST. The membranes were exposed to ECL Plus (Amersham/GE Healthcare, Pittsburg, PA) for 2–5 min and imaged using a Typhoon 9410 Variable Mode Imager (Amersham). Densitometry was performed using ImageQuant 5.2 software (Molecular Dynamics, Pittsburg, PA). All secondary antibodies were purchased from Santa Cruz Biotechnologies (Santa Cruz, CA). The following primary antibodies from Santa Cruz Biotechnology were used: TIA-1 (goat polyclonal), Grp78/BiP (mouse monoclonal), Actin (goat polyclonal), GAPDH (mouse monoclonal) and ATF4 (rabbit polyclonal). The eIF2 α (rabbit polyclonal) and p-eIF2 α (rabbit polyclonal) were purchased from Cell Signaling (Danvers, MA).

Taqman real time PCR (RT-PCR)

DU-145 cells were grown on 10 cm plates (Corning) to 80 % confluency at least 24 h prior to treatment. Cells were treated with BA and analyzed at various time points. RNA was isolated from cells using an RNeasy mini kit (Qiagen, Valencia, CA). Total RNA (2 μg) was reverse transcribed using Superscript III Reverse Transcriptase (Invitrogen) with random hexamer primers (Life Technologies) at a final volume of 20 μl at 25 °C, 10 min (10:00); 50 °C, 45:00; and 70 °C, 15:00. Applied Biosystems (ABI, Foster City, CA) Taqman predesigned assays were used for all

genes as well as GAPDH as a control internal housekeeping gene. Plates were read by a 7500 Fast Real Time PCR System using the 7500 Fast System Software v1.4.0 (ABI). Quantitation of gene expression levels were calculated from a standard curve created from reactions containing a combination of cDNA from all treatments for each gene.

Cell cycle analysis

Flow cytometry was performed to determine if BA caused a shift in cell cycle to the G1 phase. DU-145 cells were treated with 0 and 50 μM BA for 24 h. The cells were washed with PBS, scraped from the plate with a rubber policeman, centrifuged for 5 min at 1,200 rpm, and resuspended in 1 ml of DNA staining hypotonic propidium iodide solution (1 mg/ml sodium citrate, 0.3 % tritonX100, 100 $\mu\text{g}/\text{ml}$ propidium iodide, 20 $\mu\text{g}/\text{ml}$ ribonuclease A). The cells were incubated for 30 min followed by cell cycle analysis using a FACS Calibur Flow Cytometer with Modfit LT 3.0 software for data analysis. Analysis of each sample was performed on greater than 10,000 events and coefficients of variation less than 5 %.

Statistical analysis

All immunoblot were analyzed using the unpaired Student's *t* test. All time points represent 3–6 replicates. ImageJ software (NIH, Bethesda, MD) was used for immunofluorescence quantitation. Cells with clear borders between the nucleus and cytoplasm were selected for analysis. The intensity of areas of equal size in the nucleus and cytoplasm was quantified using the histogram tool in RGB mode. RT-PCR data points represent 3–6 replicates and were analyzed using the unpaired Student's *t*-test.

Results

BA causes dose-dependent changes in ER morphology

Light microscopy analysis of BA treated DU-145 cells showed cell flattening (Barranco and Eckhart 2006), therefore we were interested in knowing how this morphological change manifested at the ultrastructural level. We used TEM on DU-145 cells treated for 24 h with 0, 10, 50 or 250 μM BA. The results show a

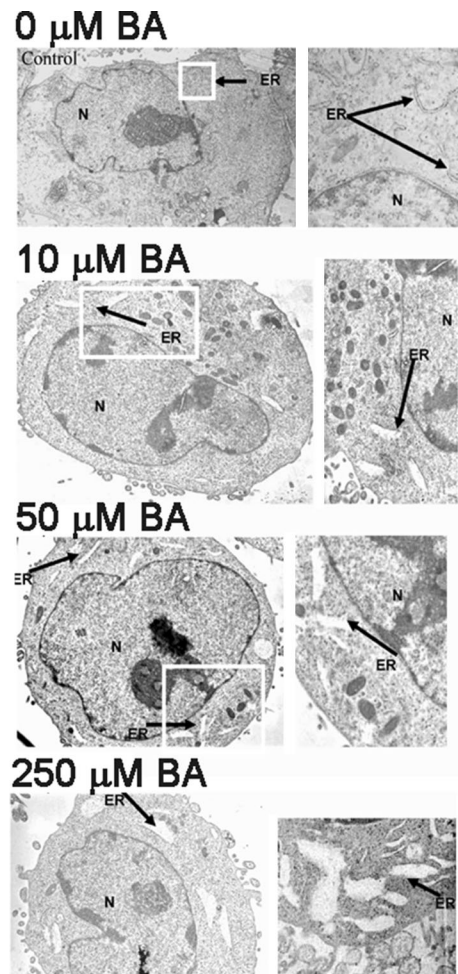


Fig. 1 BA induces ER vacuolization and expansion in DU-145 cells. TEM images of DU-145 cells treated for 24 h with 0, 10, 50, and 250 μM BA ($n = 3$). Cells exhibited a dose-dependent swelling and vacuolization of the ER, (*N* nucleus, *ER* endoplasmic reticulum). *White boxes* indicate magnified area shown on the *right*

dose-dependent increase in ER expansion, cytoplasmic granularity and cytoplasmic vacuole formation (Fig. 1).

BA induces phosphorylation of eIF2 α and the formation of cytosolic stress granules

Cells respond to changes in their environment by reprogramming translation to adapt to the new conditions (Kawai et al. 2004). eIF2 α is the regulatory subunit of the large ternary complex, eIF2-GTP-tRNAⁱ Met, which positions the initiator methionine at

the first codon of mRNA to commence translation and protein synthesis. Phosphorylation of eIF2 α on serine 51 inhibits the formation of the complex, thus inhibiting global translation allowing cells to recover from ER stress (Zoll et al. 2002). We observed an increase in phosphorylation of eIF2 α from 1 to 3 h following treatment of DU-145 cells with 50 μ M BA (Fig. 2a). We used thapsigargin as positive control since it induces ER stress by decreasing ER luminal Ca²⁺. Thapsigargin also significantly activated phosphorylation of eIF2 α in DU-145 cells at 24 h (Fig. 2a).

The absence of eIF2–GTP–tRNAⁱ Met results in eIF2/eIF5-deficient, ‘stalled’ 48S pre-initiation complex (Kedersha et al. 2002). The eIF2/eIF5-deficient pre-initiation complexes and their associated mRNA transcripts are routed to cytoplasmic stress granules (SG) in a process that requires the RNA-binding proteins T-cell intracellular antigen-1 (TIA-1) and TIAR (Anderson and Kedersha 2002). TIA-1 normally resides in the nucleus of unstressed cells but under stress conditions is recruited into SGs. Nearly 90 % of TIA-1 and about 50 % of cytoplasmic poly(A) RNA and poly(A)-binding protein-1 is recruited into SGs (Anderson and Kedersha 2002; Kedersha et al. 2002). We treated cells with 10 μ M BA or thapsigargin as a positive control and used a polyclonal antibody to TIA-1 to positively identify cytoplasmic granules as SG. TIA-1 translocation from the nucleus began to occur 15 min after treatment and reached a maximum by 1 h (Fig. 3). This correlated with the timing of 1 h maximum for eIF2 α phosphorylation (Fig. 2a).

BA treatment increases GRP78/BiP

Glucose-regulated protein binds to and maintains the transmembrane sensor PERK in an inactive form (Hendershot 2004; Pfaffenbach and Lee 2011). GRP78/BiP protein levels significantly increased in DU-145 cells treated with 50 μ M BA for 6, 12 and 24 h post-treatment (Fig. 2b).

BA induces ATF4

Phosphorylation of eIF2 α activates synthesis of ATF4, a transcription factor in the highly conserved ISR that enables cells to adapt to changing environmental conditions. We used polyclonal antibodies to measure ATF4 protein and observed an increase at 24 h in cells treated with 10 μ M BA (Fig. 2c). The results of a dose

response study showed the expression of ATF4 mRNA was increased by treatment with 10, 50 and 100 μ M BA, but not 1 μ M BA (Fig. 2d). A time course study showed the expression of ATF4 mRNA in cells treated with 10 μ M BA was higher at 30 min, 1 and 2 h post treatment (Fig. 2e). ATF4 mRNA levels returned to normal in the interval between 4 and 12 h and increased again at 24 h.

Cell cycle percentages were not affected by a 24 h treatment of BA

Flow cytometry analysis following a 24 h treatment with 50 μ M BA had little impact on the cell cycle. The percent of cells treated with 0 or 50 μ M BA were: G1 phase 50.59 \pm 0.75 and 51.21 \pm 0.62 %, S phase 13.09 \pm 1.16 and 15.15 \pm 0.38 %, G2 phase 32.09 \pm 0.46 and 31.53 \pm 0.18 % respectively (Fig. 4). The 2 % shift in S phase (p value = 0.03) was so small it was doubtful it had biological meaning. This result is consistent with previous reports demonstrating that BA does not cause a biologically significant effect on the cell cycle (Barranco and Eckhart 2004; Bradke et al. 2008). We did not observe an apoptotic cell population after BA treatment.

Discussion

A review conducted by the Institute of Medicine of the available data on dietary boron concluded it was beneficial but the molecular mechanisms underpinning its positive effects were unknown (IOM 2001). We describe in this article molecular responses of DU-145 human prostate cancer cells that follow treatment with physiological concentrations of BA. We draw several conclusions from our experimental results.

First, BA causes a dose- and time-dependent expansion of the ER with formation of cytoplasmic SGs (Figs. 1, 2). We positively identified cytosolic granules as SGs using an antibody to the tumor suppressor TIA-1, a classic biomarker of SG formation (Kedersha et al. 1999). TIA-1, with TIAR, act downstream of p-eIF2 α to promote the recruitment of untranslated mRNAs into SGs which are essential in regulating developmental and stress-responsive pathways at the level of alternative pre-mRNA splicing and mRNA translation (Kedersha et al. 1999; Buchan and Parker 2009; Bauer et al. 2012). This allows for

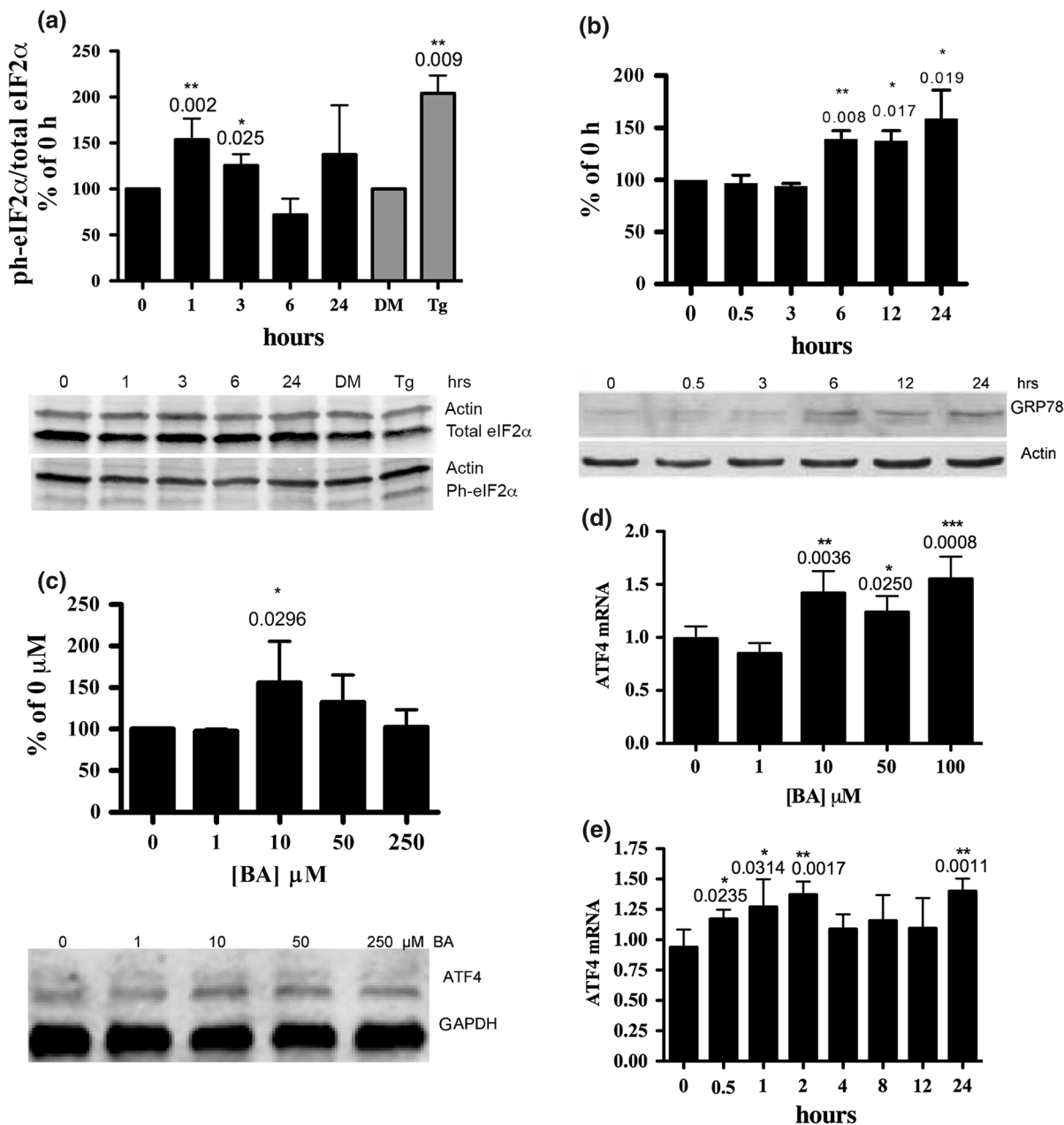


Fig. 2 BA induces the eIF2 α /ATF4 pathway. **a** 50 μ M BA treated for 24 h induced phosphorylation of eIF2 α in DU-145 cells at 1, and 3 h of treatment ($n = 3-5$). DU-145 cells treated with 1 μ M thapsigargin (Tg) or DMSO (DM) for 1 h, $n = 3$. **b** DU-145 cells treated with 50 μ M BA for 0, 0.5, 3, 6, 12 and 24 h. GAPDH was used as an internal loading control. Translation of GRP78/BiP increased in cells treated at 6–24 h, ($n = 3-4$). **c** Treatment of DU-145 cells with 10 μ M BA for 24 h caused a significant increase in ATF4. **d** DU-145 cells were

treated with different doses of BA for 24 h and ATF4 mRNA levels measured using real-time PCR ($n = 3-6$). Significant increases in mRNA were observed at 10, 50 and 100 μ M BA. **e** A time course study following treatment of DU-145 cells with 10 μ M BA showed significantly higher ATF4 mRNA levels at 0.5, 1, 2, and 24 h ($n = 3-6$). Significance differences from 0 concentration or time are shown and represented using * $p < 0.05$, ** $p < 0.01$ and *** $p < 0.001$. Error bars represent standard deviations

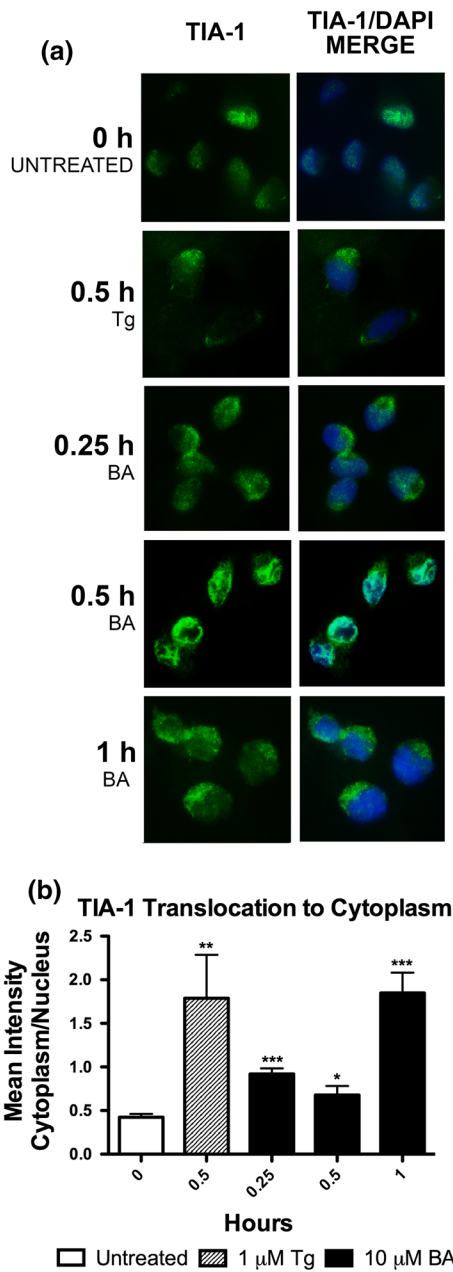


Fig. 3 BA induces formation of TIA-1 positive stress granules. 10 μM BA induced formation of TIA-1 positive stress granules in DU-145 cells at 0.25, 0.5, and 1 h, indicated by TIA-1 protein (green) moving out of the nucleus (blue) with BA treatment. 1 μM thapsigargin (Tg) was used as a positive control, (n = 6–24 cells). All time points showed a significant increase. Pictures are representative of results. Significance differences were represented as *p < 0.05, **p < 0.01, and ***p < 0.001 and error bars represent standard deviations. (Color figure online)

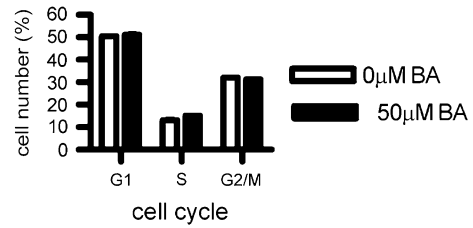


Fig. 4 The cell cycle was not significantly altered by BA treatment. Flow cytometry analysis was conducted a 24 h treatment with 0 or 50 μM BA. The percent of cells treated with 0 or 50 μM BA were: G1 phase 50.59 ± 0.75 and 51.21 ± 0.62 %, S phase 13.09 ± 1.16 and 15.15 ± 0.38 %, G2 phase 32.09 ± 0.46 and 31.53 ± 0.18 % respectively, (n = 3). The 2 % shift in S phase was of doubtful biological significance. Standard deviation error bars were plotted, but are too close to the bar graph to visualize

temporary confinement of mRNA transcripts and reduces their ability to interact with other molecules while preventing their degradation (Buchan and Parker 2009). Activation of TIA-1 in HeLa cells has been shown to prevent cell proliferation, tumor growth, and invasion (Izquierdo et al. 2011). Our observation that BA activates TIA-1 in DU-145 cells suggests this is part of the mechanism that underpins BA’s chemopreventive and biological activity. The ability of BA to activate TIA-1 provides insight into a potential mechanism underlying BA stimulated increases in TNFα in human fibroblasts and pigs (Armstrong and Spears 2003; Benderdour et al. 1998). TIA-1 is a component of a regulatory complex that binds to an adenine/uridine-rich element in the 3’UTR of TNFα mRNA. TIA-1 binding represses TNFα mRNA translation under non-stress conditions, but releases it during ER stress (Gueydan et al. 1999; Piecyk et al. 2000). Our results suggest BA may induce TNFα by causing TIA-1 to translocate from the nucleus to stress granules in the cytoplasm, thus removing its repressive effect (Benderdour et al. 1998; Armstrong and Spears 2003).

Second, BA increases eIF2α phosphorylation and BiP/GRP78 translation. BiP/GRP78 inactivates PERK and is the major ER Ca²⁺ storage protein and is regulated by luminal Ca²⁺ levels (Lievremont et al. 1997). BIP/GRP78 is released and PERK is activated and phosphorylates eIF2α when luminal Ca²⁺ levels fall, (Lievremont et al. 1997). Our results show

phosphorylation of eIF2 α is a time-dependent response that peaks 1 h post-treatment which is within the time frame reported for BA to decrease ER Ca²⁺ in DU-145 cells (Henderson et al. 2009).

Third, BA upregulates the transcription factor, ATF4. Phosphorylation of eIF2 α increases upstream open reading frame (uORF) mediated translation of bone related activating transcription factor 4 (ATF4) (Vattem and Wek 2004). The ph-eIF2 α /ATF4 pathway is highly conserved from yeast to mammals and has been named the ISR because it is a target of many different types of environmental stresses (Harding et al. 2003). Our observation that BA induces mild activation of ATF4 in prostate cancer cells may provide insight for understanding how boron supplementation increases bone mass and strength (Hunt 1996; Armstrong and Spears 2003; Nielsen and Stoecker 2009). Mild activation of ATF4 regulates osteogenesis during development and postnatally regulates bone remodeling and the osteoblast specific gene osteocalcin (Wang et al. 2012). Parathyroid hormone mediates its functions in part by regulating binding of ATF4 to osteocalcin which is an essential regulator of endochondral bone formation and for the reversal of bone loss and (Danciuk et al. 2012).

In summary, previous work has shown that BA is a competitive inhibitor of cADPR induced Ca²⁺ release from the ryanodine receptor, and decreases ER Ca²⁺ (Henderson et al. 2009). In this paper we demonstrate that mild ER stress and activation of the ISR, both known to be initiated by ER Ca²⁺ depletion, occur following treatment of DU-145 prostate cancer cells with physiological concentrations of BA. In the context of the literature, our present findings suggest mild ER stress with mild activation of the eIF2 α /ATF pathway may underpin the anticarcinogenic and bone strengthening effects of boron.

Acknowledgments UC Toxic Substances and Training Grant to the UCLA Molecular Toxicology Program provided partial support for KH, SK and KY. Other support was provided by personal funds from CE.

Conflict of interest The authors had no conflict of interest in undertaking this project.

Open Access This article is distributed under the terms of the Creative Commons Attribution License which permits any use, distribution, and reproduction in any medium, provided the original author(s) and the source are credited.

References

- Anderson P, Kedersha N (2002) Stressful initiations. *J Cell Sci* 115:3227–3234
- Armstrong TA, Spears JW (2003) Effect of boron supplementation of pig diets on the production of tumor necrosis factor- α and interferon- γ . *J Anim Sci* 81:2552–2561
- Barranco WT, Eckhart CD (2004) Boric acid inhibits prostate cancer cell proliferation. *Cancer Lett* 216:21–29
- Barranco W, Eckhart C (2006) Cellular changes in boric acid-treated DU-145 prostate cancer cells. *Br J Cancer* 94:884–890
- Barranco W, Hudak P, Eckhart C (2007a) Evaluation of ecological and in vitro effects of boron on prostate cancer risk. *Cancer Causes Control* 18:71–77. doi:10.1007/s10552-006-0077-8
- Barranco W, Hudak P, Eckhart CD (2007b) Erratum: evaluation of ecological and in vitro effects of boron on prostate cancer risk. *Cancer Causes Control* 18:583–584. doi:10.1007/s10552-007-9023-7
- Bauer WJ, Heath J, Jenkins JL, Kielkopf CL (2012) Three RNA recognition motifs participate in RNA recognition and structural organization by the pro-apoptotic factor TIA-1. *J Mol Biol* 415:727–740. doi:10.1016/j.jmb.2011.11.040
- Benderdour M, Hess K, Dzondo-Gadet M, Nabet P, Belleville F, Dousset B (1998) Boron modulates extracellular matrix and TNF alpha synthesis in human fibroblasts. *Biochem Biophys Res Commun* 246:746–751
- Bennett A, Rowe RI, Soch N, Eckhart CD (1999) Boron stimulates yeast (*Saccharomyces cerevisiae*) growth. *J Nutr* 129:2236–2238
- Berridge MJ (1997) Elementary and global aspects of calcium signalling. *J Exp Biol* 200:315–319
- Berridge MJ (2002) The endoplasmic reticulum: a multifunctional signaling organelle. *Cell Calcium* 32:235–249
- Bolt HM, Basaran N, Duydu Y (2012) Human environmental and occupational exposures to boric acid: reconciliation with experimental reproductive toxicity data. *J Toxicol Environ Health Part A* 75(8–10):508–514. doi:10.1080/15287394.2012.675301
- Bradke TM, Hall C, Carper SW, Plopper GE (2008) Phenylboronic acid selectively inhibits human prostate and breast cancer cell migration and decreases viability. *Cell Adhes Migr* 2:153–160
- Buchan JR, Parker R (2009) Eukaryotic stress granules: the ins and outs of translation. *Mol Cell* 36:932–941. doi:10.1016/j.molcel.2009.11.020
- Chapin RE, Ku WW, Kenney MA, McCoy H, Gladen B, Wine RN, Wilson R, Elwell MR (1997) The effects of dietary boron on bone strength in rats. *Fundam Appl Toxicol* 35:205–215
- Conn PM (2011) Methods in enzymology, vol 489. The unfolded protein response and cellular stress, part A. Academic Press, London
- Danciuk TE, Li Y, Koh A, Xiao G, McCauley LK, Franceschi RT (2012) The basic helix loop helix transcription factor Twist1 is a novel regulator of ATF4 in osteoblasts. *J Cell Biochem* 113:70–79. doi:10.1002/jcb.23329

- Deniaud A, Sharaf el dein O, Maillier E, Poncet D, Kroemer G, Lemaire C, Brenner C (2008) Endoplasmic reticulum stress induces calcium-dependent permeability transition, mitochondrial outer membrane permeabilization and apoptosis. *Oncogene* 27(3):285–299. doi:[10.1038/sj.onc.1210638](https://doi.org/10.1038/sj.onc.1210638)
- EPA (2004) Toxicological review of boron and compounds (CAS No. 7440-42-8). U.S. Environmental Protection Agency, Washington, DC
- Gueydan C, Droogmans L, Chalon P, Huez G, Caput D, Kruijs V (1999) Identification of TIAR as a protein binding to the translational regulatory AU-rich element of tumor necrosis factor α mRNA. *J Biol Chem* 274:2322–2326
- Harding H, Zhang Y, Zeng H, Novoa I, Lu P, Calfon M, Sadri N, Yun C, Popko B, Paules R, Stojdl D, Bell J, Hettmann T, Leiden J, Ron D (2003) An integrated stress response regulates amino acid metabolism and resistance to oxidative stress. *Mol Cell* 11:619–633
- Hendershot LM (2004) The ER chaperone BiP is the master regulator of ER function. *Mt Sinai J Med* 71:289–297
- Henderson KA (2009) Boric acid localization and effects on storage calcium release and the endoplasmic reticulum in prostate cancer cells. Dissertation, University of California Los Angeles
- Henderson KA, Eckhart CD (2006) Boric acid induces ER stress and UPR in human prostate DU-145 and LNCaP cancer cells. *FASEB J* 20:A560
- Henderson K, Stella SL, Kobylewski S, Eckhart CD (2009) Receptor activated Ca^{2+} release is inhibited by boric acid in prostate cancer cells. *PLoS ONE* 4:e6009. doi:[10.1371/journal.pone.0006009](https://doi.org/10.1371/journal.pone.0006009)
- Hunt C (1996) Biochemical effects of physiological amounts of dietary boron. *J Trace Elem Res* 9:185–213
- IOM (2001) A Report of the Panel on micronutrients, subcommittees on upper reference levels of nutrients and of interpretation and use of dietary reference intakes, and the Standing Committee on the Scientific Evaluation of Dietary Reference Intakes. Institute of Medicine
- Izquierdo JM, Alcalde J, Carrascoso I, Reyes R, Ludena MD (2011) Knockdown of T-cell intracellular antigens triggers cell proliferation, invasion and tumour growth. *Biochem J* 435:337–344. doi:[10.1042/BJ20101030337](https://doi.org/10.1042/BJ20101030337)
- Johnson SL, Smith KW (1976) The interaction of borate and sulfite with pyridine nucleotides. *Biochemistry* 15:553–559
- Kawai T, Fan J, Mazan-Mamczarz K, Gorospe M (2004) Global mRNA stabilization preferentially linked to translational repression during the endoplasmic reticulum stress response. *Mol Cell Biol* 24:6773–6787
- Kedersha NL, Gupta M, Li W, Miller I, Anderson P (1999) RNA-binding proteins TIA-1 and TIAR link the phosphorylation of eIF-2 α to the assembly of mammalian stress granules. *J Cell Biol* 147:1431–1441
- Kedersha N, Chen S, Gilks N, Li W, Miller I, Stahl J, Anderson P (2002) Evidence that ternary complex (eIF2-GTP-tRNA-Met)-deficient preinitiation complexes are core constituents of mammalian stress granules. *Mol Biol Cell* 13:195–210
- Kim D, Marbois B, Faull K, Eckhart C (2003) Esterification of borate with NAD^{+} and $NADH$ as studied by electrospray ionization mass spectrometry and ^{11}B NMR spectroscopy. *J Mass Spectrom* 38:632–640
- Kim D, Faull K, Norris A, Eckhart C (2004) Borate–nucleotide complex formation depends on charge and phosphorylation state. *J Mass Spectrom* 39:743–751
- Kim D, Que Hee S, Norris A, Faull K, Eckhart C (2006) Boric acid inhibits ADP-ribosyl cyclase non-competitively. *J Chromatogr A* 1115:246–252
- Korkmaz M, Uzgoren S, Bakırdere S, Aydin F, Ataman OY (2007) Effects of dietary boron on cervical cytopathology and on micronucleus frequency in exfoliated buccal cells. *Environ Toxicol* 22:17–25. doi:[10.1002/tox.20229](https://doi.org/10.1002/tox.20229)
- Ku WW, Chapin RE, Wine RN, Gladen BC (1993) Testicular toxicity of boric acid (BA): relationship of dose to lesion development and recovery in the F344 rat. *Reprod Toxicol* 7:305–319
- Lievremont JP, Rizzuto R, Hendershot L, Meldolesi J (1997) BiP, a major chaperone protein of the endoplasmic reticulum lumen, plays a direct and important role in the storage of the rapidly exchanging pool of Ca^{2+} . *J Biol Chem* 272:30873–30879
- Mahabir S, Spitz M, Barrera S, Dong Y, Eastham C, Forman M (2008) Dietary boron and hormone replacement therapy as risk factors for lung cancer in women. *Am J Epidemiol* 167:1070–1080
- Narotsky MG, Schmid JE, Andrews JE, Kavlock RJ (1998) Effects of boric acid on axial skeletal development in rats. *Biol Trace Elem Res* 66:373–394
- Nielsen FH, Stoecker BJ (2009) Boron and fish oil have different beneficial effects on strength and trabecular microarchitecture of bone. *J Trace Elem Med Biol* 23:195–203
- Pfaffenbach KT, Lee AS (2011) The critical role of GRP78 in physiologic and pathologic stress. *Curr Opin Cell Biol* 23:150–156
- Pieczek M, Wax S, Beck A, Kedersha N, Gupta M, Maritim B, Chen S, Gueydan C, Kruijs V, Streuli M, Anderson P (2000) TIA-1 is a translational silencer that selectively regulates the expression of TNF α . *EMBO J* 19:4154–4163
- Rainey C, Nyquist L (1998) Multicountry estimation of dietary boron intake. *Biol Trace Elem Res* 66:79–86
- Shen X, Zhang K, Kaufman RJ (2004) The unfolded protein response—a stress signaling pathway of the endoplasmic reticulum. *J Chem Neuroanat* 28(1–2):79–92
- So AY-L, de la Fuente E, Walter P, Shuman M, Bernales S (2009) The unfolded protein response during prostate cancer development. *Cancer Metastasis Rev* 28:219–223. doi:[10.1007/s10555-008-9180-5](https://doi.org/10.1007/s10555-008-9180-5)
- Ulusik I, Kaya A, Formenko DE, Karakaya HC, Carlson BA, Gladyshev VN, Koc A (2011) Boron stress activates the general amino acid control mechanism and inhibits protein synthesis. *PLoS ONE* 6:e27772. doi:[10.1371/journal.pone.0027772](https://doi.org/10.1371/journal.pone.0027772)
- Vattem KM, Wek RC (2004) Reinitiation involving upstream ORFs regulates ATF4 mRNA translation in mammalian cells. *Proc Natl Acad Sci USA* 101:11269–11274. doi:[10.1073/pnas.0400541101](https://doi.org/10.1073/pnas.0400541101)
- Wang W, Lian N, Ma Y, Li L, Gallant RC, Eliftheriou F, Yang X (2012) Chondrocytic ATF4 regulates osteoblast differentiation and function via Ihh. *Development* 139:601–611. doi:[10.1242/dev.069575](https://doi.org/10.1242/dev.069575)
- WHO (1998) Boron, Environmental Health Criteria 204. International Programme on Chemical Safety. World Health Organization, Geneva
- Zoll WL, Horton LE, Komar AA, Hensold JO, Merrick WC (2002) Characterization of mammalian eIF2A and identification of the yeast homolog. *J Biol Chem* 277:37079–37087